

# 1 Time-reversal focusing of therapeutic ultrasound on targeted microbubbles

2 Olivier Couture,<sup>1,2,a)</sup> Jean-François Aubry,<sup>1</sup> Mickael Tanter,<sup>1,3</sup> and Mathias Fink<sup>1</sup>

3 <sup>1</sup>Institut Langevin Ondes et Images (CNRS UMR 7587), ESPCI, Paris 75005, France

4 <sup>2</sup>Fondation Pierre-Gilles de Gennes, France

5 <sup>3</sup>INSERM, France

6 (Received 29 October 2008; accepted 6 April 2009; published online xx xx xxxx)

AQ:  
#1

7 Targeted microbubbles bind specifically to molecular markers of diseases and their unique acoustic  
8 signature is used to image cellular processes *in vivo*. The ability of time-reversal processing to focus  
9 waves through heterogeneities on such targeted microbubbles is demonstrated. For this purpose,  
10 microbubbles were deposited on a gelatin phantom and their specific signal was recorded by a high  
11 intensity ultrasonic array. The amplified time-reversed signal was re-emitted and shown to focus  
12 back in the region where the bound microbubbles were present. This proof of concept emphasizes  
13 that molecular-time-reversal focusing could guide energy deposition on early, diffuse, or metastatic  
14 disease. © 2009 American Institute of Physics. [DOI: 10.1063/1.3126039]

15  
16 Ultrasound therapy can treat various pathologies such as  
17 solid tumors, arteriosclerosis, and hemorrhage.<sup>1</sup> Absorption  
18 of ultrasound energy not only leads to tissue heating but also  
19 to cavitation and sonoporation.<sup>2</sup> These effects can necrose  
20 tissue or induce apoptosis,<sup>3</sup> facilitate the passage of drugs<sup>4</sup> or  
21 erode thrombi *in vivo*.<sup>5</sup> In homogeneous media, the energy  
22 deposition is optimal at the focus of the ultrasonic trans-  
23 ducer, determined either by the geometry of the source or the  
24 electronic delays applied on the elements of an array. The  
25 focal zone can be placed deep into tissue and moved to treat  
26 a diseased region highlighted by prior ultrasound imaging,  
27 magnetic resonance imaging, or computed tomography.  
28 However, these imaging methods are, currently, mainly sen-  
29 sitive toward changes in physical properties of tissues. Treat-  
30 ment based on the molecular and cellular processes underly-  
31 ing cancer and arteriosclerosis are likely to be more specific  
32 to the early onset of these diseases.

33 Such molecular specificity has been attained in ultra-  
34 sound imaging by exploiting targeted contrast agents.<sup>6</sup> These  
35 agents, usually bubbles a few microns in diameter, are re-  
36 tained in a tumor or thrombus through the antibodies or  
37 ligands present on their surface. These microbubbles have a  
38 specific acoustic response allowing ultrasound imaging to  
39 distinguish them from tissue or blood. For instance, mi-  
40 crobubbles emits detectable harmonics when insonified by a  
41 monochromatic incident wavefield.<sup>7</sup> They can also be dis-  
42 ruptured, which makes differentiation techniques very sensitive  
43 to microbubbles.<sup>8</sup> In fact, the ultrasound signature of a single  
44 bound microbubble can be detected.<sup>9</sup> Targeting of these con-  
45 trast agents causes these echoes to originate from a region of  
46 disease-specific molecular expression.

47 The Laboratoire Ondes et Acoustique previously ex-  
48 ploited time-reversal acoustics<sup>10,11</sup> to focus waves on cavi-  
49 tation bubbles induced within tissue.<sup>12</sup> This method was shown  
50 to efficiently correct aberrations and improve focusing of ul-  
51 trasound therapy. A similar technique can be applied to tar-  
52 geted contrast agents. Using the ability of time-reversal to  
53 refocus an amplified ultrasound wave toward its initial  
54 source, we present a method to restrict energy deposition on  
55 localized or extended areas of specific biomarkers expres-

56 sion. Beyond the important issue of specificity, targeted con-  
57 trast agents could also provide an efficient way to correct for  
58 beam aberrations induced by heterogeneities encountered by  
59 the wave on its travel path. An *in vitro* targeting phantom  
60 was designed to demonstrate specific focusing of ultrasound  
61 on bound microbubbles (Fig. 1). Gelatin (5%) and biotin  
62 (1%) were mixed into water and poured in plastic Petri  
63 dishes. Microbubbles covered with avidin (Bracco Research  
64 SA) were diluted (1/10), mixed with black ink and deposited  
65 as 15  $\mu$ l droplet on the gel surface.<sup>13</sup> The microbubbles in-  
66 teracted with the surface of the gel through the avidin-biotin  
67 complex and, after washing, left a disk 5 mm in diameter  
68 populated with bound microbubbles. Surface density of mi-  
69 crobubbles was estimated to attain 70 microbubbles/mm<sup>2</sup>.<sup>13</sup>  
70 The plates were then installed in a water tank such that the  
71 gelatin surface was coplanar with the focal plane of a 70-  
72 elements high-intensity focused ultrasound array. Each ele-

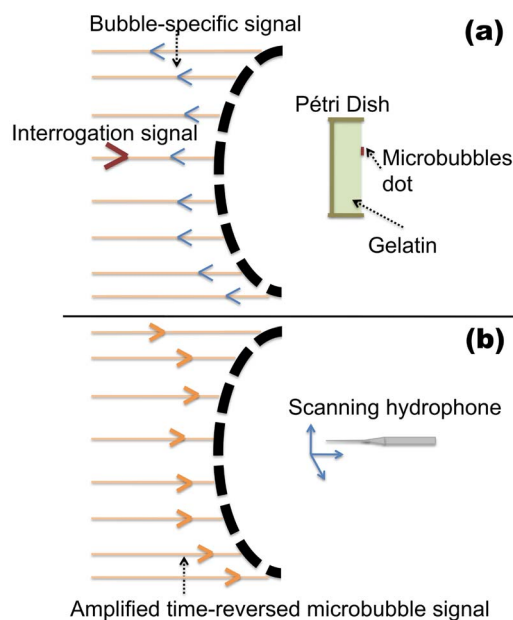


FIG. 1. (Color online) Time-reversal on a dot of microbubbles. (a) The echo of an interrogation pulse is collected before and after the disruption of the microbubbles. (b) The time-reversed signal of the microbubbles is amplified, emitted, and measured by a hydrophone.

<sup>a)</sup>Electronic mail: olicou@gmail.com.

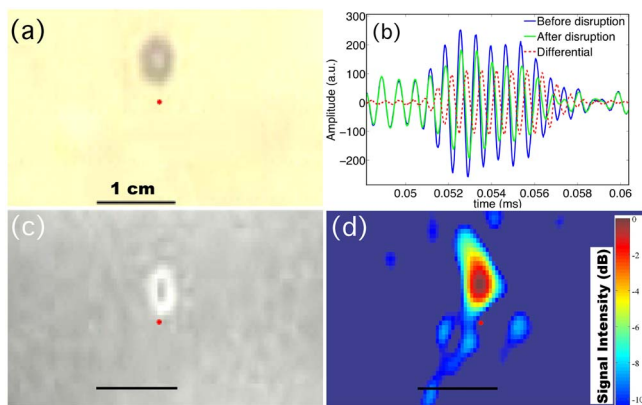


FIG. 2. (Color online) (a) Photograph of the dyed microbubbles dot. (b) Echo of a weak interrogation pulse on the gelatin surface on a single element. (c) Photograph of the color change on the thermosensitive paper. (d) Acoustic field collected by the hydrophone. The red dot is the geometric focal point, the black line is 10 mm long and the colorbar scale is dB relative to the maximum.

AQ:  
#5

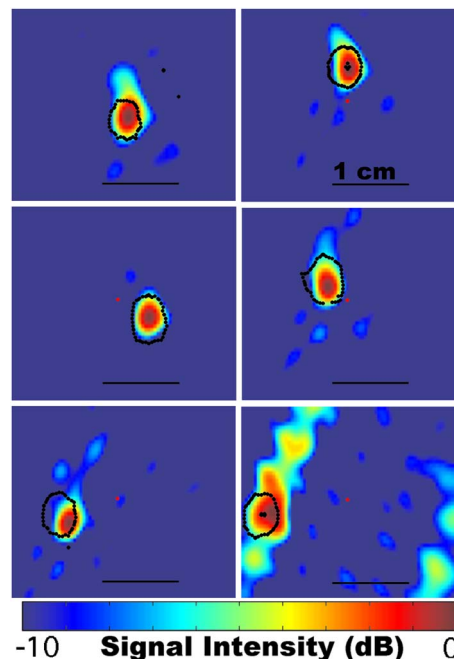


FIG. 3. (Color online) Acoustic field collected by the hydrophone for dots of microbubbles at different positions. The colorbar scale is dB relative to the maximum. The black border corresponds to the position of the microbubbles dot as observed optically.

ment of the array were emitter-receiver tuned at 1 MHz and driven by a fully programmable electronic board relying on a 30 MHz sampling frequency analog transmitter. A micrometric step motor moved the microbubbles dots with respect to the geometric focus of the transducer to determine steering capabilities.

The specific signal of the microbubbles was collected through their disruption. At first, a low pressure imaging pulse was emitted by a single transducer to avoid *a priori* focusing. The corresponding echoes from the plate and the microbubbles were collected by the entire array. Then, a high amplitude pulse was emitted by a high intensity focused ultrasound array, with sufficient pressure to disrupt the microbubbles (1.5 MPa). Finally, a new series of imaging pulses were collected. The difference between the signals before and after disruption was assumed to be specific to microbubbles [Fig. 2(b)]. These differential signals were recorded and saved. The experiment was reproduced for several positions of the microbubbles dot within the acoustic field and for several patterns of dots. This differential sequence of ultrasonic insonifications was performed in a few milliseconds and would thus be insensitive to motion artifacts in a clinical configuration.

The position of the dots of microbubbles was recorded with a camera aligned along the transducer axis. Figure 2(a) shows a picture of the disk of dyed microbubbles with respect to the focal point of the transducer. Such pictures were thresholded and the patterns were used as an overlay on the acoustic field measurement displayed in Figs. 3 and 4.

A coarse two-dimensional (2D) mapping of the acoustic energy refocusing was made using a thermosensitive paper, which replaced the gelatin dish in the water tank. The recorded echoes of the microbubbles, for each position, were time reversed, elongated, and amplified to create an emission pattern. These patterns were then emitted by the ultrasound array. Direct heating due to focused ultrasound waves could be detected through color changes of the thermosensitive paper. It was observed that the region of increased temperature was concomitant to the corresponding position of the microbubbles [Fig. 2(c)].

More precise acoustic measurements were performed by scanning a hydrophone (Onda, HNZ 0200) in the focal plane

of the transducer (0.4 mm steps in  $x, y$  plane). The emission patterns, only a few cycles in length, were sent and the resulting acoustic field was measured at each point. As shown in Fig. 2(d), the acoustic field is maximum in the area where the microbubbles were bound on gelatin surface. It demonstrated that ultrasound therapy can be guided by the echoes of the microbubbles.

When the microbubbles dot was moved around the geometric focus of the array, the therapeutic beam was simply redirected toward the new position (Fig. 3). In our specific experiment, the array was able to steer the beam within 1.5 cm from the geometric focus. However, this limitation, along with the observed sidelobes, depends solely on the physical characteristics of the array such as the number and geometry of the transducers, the emission frequency, the aperture and focal distance.

During molecularly targeted therapy, it is likely that the targeted microbubbles will accumulate over a region larger than the wavelength or in multiple metastasis. Figures 4(a) and 4(b) show how time-reversal manages to refocus simul-

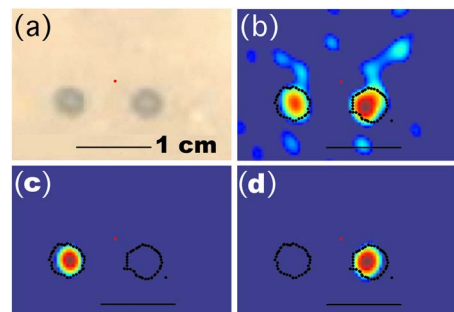


FIG. 4. (Color online) (a) Photograph of the two dyed microbubbles dot. (b) Acoustic field collected by the hydrophone. [(c) and (d)] Separation of the two microbubbles dots. Acoustic field after geometric projection and selection.

135 taneously on two separate dots of microbubbles. It empha-  
 136 sizes the ability of time-reversal processing to build a focal  
 137 pattern whose shape instantaneously fits the targeted mi-  
 138 crobubbles area. Mild temperature elevation or cavitation-  
 139 dependent effect could thus be achieved in multiple distinct  
 140 areas. However, as the treatment volume increases, part of  
 141 the antennae gain is lost and treatment time has to be in-  
 142 creased in order to accumulate sufficient thermal doses for  
 143 treatment.

144 To allow separate treatment of each dot, the treated  
 145 zones were spatially divided using beamforming. The emis-  
 146 sion pattern was convoluted with the transfer matrix acquired  
 147 in a homogeneous medium. The signals coming from the  
 148 each side of the field were separated on the resulting image  
 149 using a convolution by a 2D mask and converted back to the  
 150 emission patterns by convoluting with the transpose of the  
 151 transfer matrix. As shown in Figs. 4(c) and 4(d), these two  
 152 emission patterns focused successively on each dot and high  
 153 acoustic pressures were retrieved. More intricate pattern of  
 154 microbubbles could also be treated by selecting individual  
 155 part of the echoes and treating point-by-point. This study  
 156 demonstrated that the echoes from bound microbubbles can  
 157 be exploited for direct time-reversal ultrasound therapy.  
 158 Thus, ultrasonic heating or cavitation can be targeted to dif-  
 159 fuse or early disease based on its molecular expression and  
 160 not only on the modification of its physical properties. This  
 161 could benefit the treatment of metastasis and infiltrating tu-  
 162 mors. Moreover, contrarily to drug-carrying microbubbles,  
 163 “molecular-focusing” decouples therapeutic dose from the  
 164 contrast agents. After the bubble-specific signals are re-

corded, the technique does not require the microbubbles to 165  
 be present and the deposited energy is purely controlled by 166  
 ultrasound. Because this technique does not require prior im- 167  
 aging, it can easily be made iterative and treatment can be 168  
 repeated as long as microbubbles binds in large amounts in a 169  
 region. However, molecular-focusing is limited to highly 170  
 specific microbubbles targeting which can only improve as 171  
 our knowledge of the cellular pathways of disease progress. 172

The authors thank Bracco Research SA for kindly pro- 173  
 viding the targeted microbubbles. 174

- <sup>1</sup>G. ter Haar, *Prog. Biophys. Mol. Biol.* **93**, 111 (2007). 175 AQ:  
<sup>2</sup>C. X. Deng, F. Sieling, H. Pan, and J. Cui, *Ultrasound Med. Biol.* **30**, 519 176 #1  
 (2004). 177  
<sup>3</sup>N. Vykhodstseva, N. McDannold, and K. Hynynen, *Ultrasound Med. Biol.* **32**, 1923 (2006). 178  
<sup>4</sup>J. Choi, M. Pernot, S. A. Small, and E. Konofagou, *Ultrasound Med. Biol.* **33**, 95 (2007). 179 AQ:  
<sup>5</sup>R. J. Siegel and H. Luo, *Ultrasonics* **48**, 312 (2008). 180 #2  
<sup>6</sup>P. A. Dayton and J. J. Rychak, *Front. Biosci.* **12**, 5124 (2007). 181  
<sup>7</sup>P. N. Burns and S. R. Wilson, *Ultrasound Q.* **22**, 5 (2006). 182  
<sup>8</sup>P. N. Burns, S. R. Wilson, and D. Muradali, *Radiology* **201**, 158 (1996). 183  
<sup>9</sup>A. L. Klibanov, P. T. Rasche, M. S. Hughes, J. K. Wojdyla, K. P. Galen, 184 AQ:  
 and J. H. Wible G.H. Brandenburger, *Invest. Radiol.* **39**, 187 (2004). 185 #3  
<sup>10</sup>M. Fink, D. Cassereau, A. Derode, C. Prada, P. Roux, M. Tanter, J.-L. 186 AQ:  
 Thomas, and F. Wu, *Rep. Prog. Phys.* **63**, 1933 (2000). 187 #4  
<sup>11</sup>M. Fink, G. Montaldo, and M. Tanter, *Annu. Rev. Biomed. Eng.* **5**, 465 188  
 (2003). 189  
<sup>12</sup>M. Pernot, G. Montaldo, M. Tanter and M.Fink, *Appl. Phys. Lett.* **88**, 034102 (2006). 190  
<sup>13</sup>O. Couture, M. Sprague, E. Cherin, P. N. Burns, and F. S. Foster, *IEEE* 191  
*Trans. Ultrason. Ferroelectr. Freq. Control* **56**, 536 (2009). 192  
 193  
 194  
 195

**AUTHOR QUERIES — 057917APL**

- #1 Au: please supply the complete addresses for affiliations 2 and 3.
- #2 CrossRef reports the author should be "VYKHODTSEVA" not "Vykhodstseva" in the reference 3 "Vykhodstseva, McDannold, Hynynen, 2006".
- #3 Au: please supply full journal title, CODEN, and/or ISSN for the journal in Ref. 7
- #4 au: please check Refs. 8 & 13 for accuracy
- #5 Au: please note that although caption makes reference to color online, figures in print will appear in black and white